

the intensity of the lobes was greatest in the center and decreased monotonically with increasing scattering angle. This is indicative of a transformation from sheaflike to rodlike textures having a fibrillar morphology. This transformation was postulated to depend on surface tension effects resulting from restriction of the shrinkage of the drawn specimen during annealing. A similar result was reported by Misra and Stein.<sup>5</sup> When unconstrained drawn specimens were put into a hot water bath at 100 °C, they shrank. The degree of shrinkage of bulk specimens decreased with increasing crystallinity of the drawn specimens before annealing. This tendency was related to obstruction of the randomization of amorphous chain segments by the crystallites during the relaxation process. This suggests that there is an increase in the number of cross-linking points of the amorphous chain segments, leading to an increase of crystallinity.

**Acknowledgment.** We thank Professor Kawai, Department of Polymer Chemistry, Faculty of Engineering, Kyoto University, Japan, for valuable comments and suggestions. Thanks are also due to Dr. Inoue and Mr. Motegi, Toray Industries, Inc., Siga, for the sample used and for helpful comments. We are also grateful to Dr. R. St. John Manley, Department of Chemistry, McGill University, for his kind help with the English presentation.

## References and Notes

- (1) Matsuo, M.; Tamada, M.; Terada, T.; Sawatari, C.; Niwa, M. *Macromolecules*, preceding paper in this issue.
- (2) de Daubeny, R.; Bunn, C. W.; Brown, C. J. *Proc. R. Soc. London, Ser. A* 1954, 226, 531.
- (3) Roe, R.-J.; Krigbaum, W. R. *J. Appl. Phys.* 1964, 35, 2215.
- (4) Krigbaum, W. R.; Taga, T. *J. Polym. Sci., Polym. Phys. Ed.* 1979, 17, 393.
- (5) Misra, A.; Stein, R. S. *J. Polym. Sci., Polym. Phys. Ed.* 1979, 17, 235.

## Crystallization of the Extended Conformation from the Bulk in Solvent-Exposed Films of Isotactic Polystyrene

Pudupadi R. Sundararajan\* and Nancy J. Tyrer

Xerox Research Centre of Canada, 2480 Dunwin Drive, Mississauga, Ontario L5L 1J9, Canada. Received December 16, 1981

**ABSTRACT:** The extended conformation, with a nonstaggered tt state of skeletal bonds, occurs in gels of isotactic polystyrene (iPS). Intramolecular interaction between adjacent phenyls is predominant in this conformation. Although gels containing the extended conformation melt in the range 80–120 °C, this conformation cannot be crystallized from the bulk by annealing below  $T_m$ . It is shown that solvent molecules are required to provide the intermolecular interaction necessary for crystallization. Thus, through exposure of amorphous films of iPS to bulky hydrocarbon or substituted aromatic solvent vapor, crystallization of the extended conformation from the bulk has been achieved at room temperature. A unit cell with  $a = 21.0$ ,  $b = 16.4$ , and  $c = 30.6$  Å containing four chains and 8–16 solvent molecules has been proposed. The extended conformation can be induced by solvent exposure even in semicrystalline films already containing the threefold helical structure. Thus, it is shown that the extended conformation exists with significant perpetuation in the amorphous zones of semicrystalline films containing the threefold helical structure. Scanning electron micrographs show that the extended conformation, when crystallized, forms dendritic structures. It is suggested that the lower  $T_m$  of this structure compared to that of the threefold helical structure is due not to intramolecular instability but rather to the requirement of the presence of solvent molecules in the lattice.

## Introduction

Conformational energy calculations on isotactic polystyrene (iPS) have shown<sup>1</sup> that conformations near the tt state of adjacent skeletal bonds are not forbidden as heretofore believed. Although the perfectly staggered tt state with  $(\phi_i, \phi_{i+1}) = (0^\circ, 0^\circ)$  ( $\phi_i$  and  $\phi_{i+1}$  being the rotations defining the conformations around the skeletal bonds  $i$  and  $i + 1$ ) incurs severe overlap of adjacent phenyl groups, rotations of about 20° in  $\phi_i$  and  $\phi_{i+1}$  relieves such an overlap and the energy of the nonstaggered tt state becomes comparable to that of the gt state (which, when perpetuated, generates the familiar threefold helix with a repeat distance of 6.6 Å found in the crystalline state<sup>2</sup>). This feature was found to be common for most isotactic vinyl chains<sup>3,4</sup> bearing planar substituents, for example, for poly(methyl methacrylate), poly( $\alpha$ -methylstyrene), poly(vinyl acetate), and poly(*N*-vinylcarbazole).

The presence of the nonstaggered tt conformation of successive skeletal bonds is required to construct the double-helical structure proposed by Kusanagi et al.<sup>5</sup> for isotactic PMMA. The X-ray diffraction pattern obtained by Atkins et al.<sup>6</sup> for isotactic polystyrene gels prepared by quenching the solution in decalin was different from that of the crystalline threefold helical structure. The interim solution that they offered on the basis of a syncephalic

(head-to-head, tail-to-tail) sequence along the chain was contradicted by their <sup>13</sup>C NMR data. However, our calculations<sup>1</sup> reported in 1979 showed that the X-ray diffraction pattern from iPS gels can be interpreted by using the nonstaggered tt conformation of skeletal bonds in terms of an isotactic chain containing 12 monomers in a repeat distance of 30.6 Å. (This will be referred to as the extended conformation hereafter). In this conformation, the rise per repeat unit along the helix is 2.55 Å, which is larger than the distance between successive C $\alpha$  atoms, if tetrahedral bond angles are taken. Enlargement of the angle at the C $\alpha$  atom to 114° and that at the methylene carbon to 117.8° was necessary to minimize the energy and account for the helix parameters. This was discussed in a previous paper.<sup>1</sup> The calculations<sup>1</sup> also showed that the energy of the extended conformation is lower than that of the threefold helical conformation by about 1 kcal·mol<sup>-1</sup>. Calculations reported later by other authors<sup>7-9</sup> have confirmed the possibility of such an extended conformation for iPS.

Our recent studies<sup>10</sup> on the gelation of iPS, using several types of solvents, showed that although the gels can be obtained from several solvents, the resultant conformation of the chain depends on the stereochemistry and size of the solvent molecule. It was found that with bulky, non-

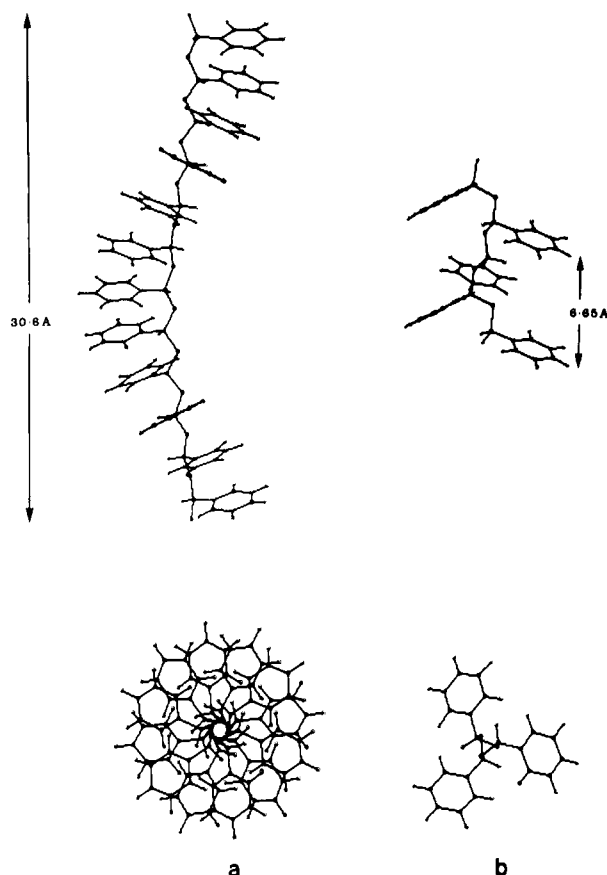


**Figure 1.** Projections of the (a) extended and (b) threefold helical conformations of isotactic polystyrene (iPS). In the extended conformation, the skeletal bonds are in the nonstaggered *tt* conformation. In the latter, the skeletal bonds follow the *tg* propagation.

planar hydrocarbon solvents, the extended conformation is obtained, whereas with aromatic solvents, a mixture of extended and threefold helical conformations or exclusively the latter resulted. This was rationalized on the basis of the accessibility of the phenyl groups for interaction with the solvent molecules and the compatibility of the latter with the phenyl groups. Examination of molecular models and Figure 1 would show that in the *tt* conformation of the meso dyad of iPS, the interaction between the adjacent phenyl groups predominates and the distance between them is not sufficient to permit entry of solvent molecules. In poor bulky solvents, such a conformation, in which short-range intramolecular interaction predominates, can be expected to occur in profusion. On the other hand, in the *tg* (or *gt*) conformation, the interaction between phenyl groups appended to adjacent  $C^\alpha$  atoms is virtually nonexistent, the phenyls are in a favorable disposition to interact with the solvent molecules, and this would be the conformation of significant population in good solvents. Thus, either conformation can be induced by an appropriate choice of solvent molecule.

Although conformational calculations<sup>1,11</sup> show that the extended conformation is accessible for iPS, its occurrence has been confirmed so far only in gels obtained by rapid quenching from high temperatures.<sup>6,10</sup> This conformation has not been reported to occur in samples crystallized from the bulk. According to the calculations,<sup>1</sup> the energy of the extended conformation is lower by about  $1000 \text{ cal}\cdot\text{mol}^{-1}$  than that of the threefold helical conformation. The gelation studies show that the melting point of such a structure varies from 60 to  $120^\circ\text{C}$ , depending on the solvent used.<sup>6,10,12</sup> In all the crystal structure studies of

iPS, however, the sample is usually annealed at temperatures above  $120^\circ\text{C}$ , where the extended conformation cannot be expected to remain. It is reasonable then to examine if the extended conformation could be obtained by annealing amorphous films at temperatures ranging from, say, 50 to  $100^\circ\text{C}$ . Our attempts showed that annealing of amorphous films does not promote crystallization of the extended conformation.

The extended conformation involves interaction of adjacent phenyls and, as such, the intermolecular interaction can be expected to be insignificant. It is possible, however, that another agent, such as a solvent molecule, is necessary to provide the necessary interaction between the chains in order for the crystallization to occur. For example, in the case of the hemicellulose xylan, intermolecular hydrogen bonding promoted by water molecules (i.e., exposure to high relative humidity) is necessary to achieve a high degree of crystallinity.<sup>13</sup> Hence, studies on solvent-vapor-exposed iPS films were undertaken to determine if the extended conformation can be crystallized from bulk films and to observe the associated morphology. The focus is on the structural and morphological aspects, and the details of kinetics of vapor absorption are not treated here.

### Experimental Section

Two samples of iPS, denoted here by A and B, were obtained from Polysciences. These are the same as those used in the previous study.<sup>10</sup> Sample A was amorphous as received in the form of pellets, whereas sample B was a crystalline powder.  $^1\text{H}$  NMR analysis<sup>14</sup> with a Bruker WM-250 NMR spectrometer showed the isotactic dyad content of both samples to be 75–80%. It is concluded that sample A is the pelletized form of sample B.

Amorphous films for vapor exposure were obtained in two ways: (i) The samples were sandwiched between a pair of glass slides and a melt-quenched film was prepared. No external pressure was applied. (ii) A 15% (w/v) solution of the sample in toluene (ACS grade) was poured on a glass plate and a film was prepared under ambient conditions. In this case, it was necessary to melt quench sample B to destroy the initial crystallinity in order to dissolve it in toluene. The resulting films in both cases were amorphous, as determined by wide-angle X-ray diffraction.

As in the previous study,<sup>10</sup> hexahydroindan (bp  $167^\circ\text{C}$ ), cyclooctane (bp  $151^\circ\text{C}$ ), ethylbenzene (bp  $136^\circ\text{C}$ ), and nitrobenzene (bp  $210^\circ\text{C}$ ) were used for vapor exposure. All solvents were of spectroscopic grade, with the exception of nitrobenzene, which was AR grade. The films were exposed at room temperature to the solvent vapor by placing them over the mouth of a small bottle containing the solvent, and both were enclosed in a glass chamber. The time of exposure varied from 24 h to 18 days, depending on the sample and the solvent. The setup is admittedly primitive. However, the aim of this study is to identify the conformation rather than to measure the diffusion rates etc. The vapor-exposed films were dried under ambient conditions for 24 h before analysis.

The films were characterized by X-ray diffraction and scanning electron microscopy. The X-ray patterns in the wide-angle region were recorded with a box-type flat-film camera (W. Warhus & Co.). Copper  $K\alpha$  radiation ( $\lambda = 1.5418 \text{ \AA}$ ) was used. Scanning electron micrographs were obtained with an ISI super II SEM and Philips 505 SEM. Densities of the films were determined by flotation in concentrated NaCl solution at  $25^\circ\text{C}$  via appropriate dilution. Solution densities were measured with a Westphal balance. Selected values of the densities are given in Table I. The densities measured here for the melt-quenched samples agree with those reported in the literature<sup>15</sup> for amorphous samples of iPS. The density measured for a gel prepared from a *cis*-decalin-*trans*-decalin solution after drying at room temperature for a few days is also given in Table I for comparison.

### Results and Discussion

**X-ray Diffraction and Unit Cell.** The amorphous films upon exposure to solvent vapor turned opaque, which is an indication of the development of crystallinity in these

Table I  
Measured Densities of Various Films Used in This Study

sample	treatment	density, g·cm <sup>-3</sup>
A	melt quenched	1.042
A	melt quenched, exposed to hexahydroindan for 3 days	1.028
A	melt-drawn fiber	1.038
A	melt-drawn fiber, exposed to hexahydroindan for 3 days	1.034
B	melt quenched	1.058
B	melt quenched, exposed to hexahydroindan for 3 days	1.034
B	dried gel prepared from <i>cis</i> -decalin- <i>trans</i> -decalin mixture	1.037

types of films. The X-ray diffraction patterns showed that crystallization has been achieved in both samples upon exposure to any of the four solvent vapors at room temperature. The diffraction patterns of both the melt-cast and toluene-cast films were similar upon solvent exposure. The patterns from the film exposed to hexahydroindan, nitrobenzene, and cyclooctane vapor are shown in Figure 2a-c, respectively. The measured  $d$  spacings are given in Table II. It is seen that as many as 14 reflections are observed. The reflections with spacings of 20.5 and 5.1 Å, characteristic of the extended conformation,<sup>6</sup> are present. None of the other reflections correspond to the threefold helical structure, and thus all of them belong to the extended structure. This has been confirmed by their disappearance upon annealing the films at 125 °C. Annealing the films at that temperature causes the threefold helical conformation to crystallize.

The number of reflections recorded here for the extended conformation is greater than that hitherto reported for this structure. The quality of the X-ray patterns is also superior due to the virtual absence of diffuse scattering that accompanies the patterns recorded from the gels. The patterns in Figure 2 also show that crystallization of exclusively the extended form has been achieved. Although in Figure 2 there is a reflection of spacing 4.8 Å similar to that in the threefold helical structure,<sup>2</sup> the absence of any other strong reflection characteristic of the threefold form leads to the conclusions that the 4.8-Å reflection observed here corresponds to the extended conformation.

The X-ray diffraction patterns from gels of iPS reported so far have not been of sufficient quality to enable the determination of the unit cell parameters for the extended structure, other than the repeat distance along the chain (30.6 Å) and the screw symmetry.<sup>6</sup> Although only the Debye-Scherrer patterns have been recorded here, since there are as many as 14 reflections, an attempt was made to deduce the unit cell dimensions by trial and error. Identification of the reflections unambiguously in terms of layer lines is thus not possible at this time.

Since a sixfold screw axis has been ascribed to the chain via previous studies,<sup>6</sup> it is tempting to consider a hexagonal unit cell. However, none of the hexagonal unit cells tested were able to index all of the observed reflections. On the other hand, all the reflections could be indexed by using an orthorhombic unit cell with  $a = 21.0$ ,  $b = 16.4$ , and  $c = 30.6$  Å. The indices of the reflections based on this unit cell are also given in Table II. With the above orthorhombic unit cell, the calculated density would be 1.58, 1.18, and 0.79 g·cm<sup>-3</sup> for eight, six, and four chains, respectively, per cell. The first two are far greater than the measured density. In systems of this type, it is not unusual to find occluded solvent molecules in the unit cell. The studies of Atkins et al.<sup>16</sup> have shown that normally in the gels of iPS the solvent molecule can be removed only by

Table II  
Observed and Calculated Interplanar Spacings

reflection no.	$d(\text{obsd})$ , Å	$d(\text{calcd})$ , Å	Miller indices ( $hkl$ )
1	21.0	21.0	100
2	16.4	16.4	010
3	13.04	12.92	110
4	10.43	10.50	200
5	8.12	8.20	020
6	7.02	7.00	300
		6.93	014
7	6.02	5.93	312
		5.95	222
		6.11	123
8	5.25	5.32	320
		5.29	130
		5.25	400
		5.24	321
9	5.04	5.1	006
10	4.79	4.85	230
		4.79	231
		4.75	412
		4.82	033
		4.72	323
		4.78	125
11	4.46	4.42	420
		4.49	413
		4.45	034
		4.44	315
		4.44	225
		4.42	216
12	3.58	3.54	340
		3.63	522
		3.51	523
		3.55	433
		3.58	243
		3.61	044
		3.59	514
		3.56	144
		3.58	425
		3.52	335
		3.57	416
13	3.07	3.66	406
		3.13	250
		3.11	251
		3.07	252
		3.08	443
		3.01	054
		3.05	534
		3.06	345
		3.06	246
		3.04	436
14	2.95	2.93	540
		2.97	350
		2.96	351
		2.92	541
		2.92	352
		2.99	253
		2.98	444
		2.98	154
		2.90	254
		2.92	535
		2.91	346

Table III  
Calculated Densities for Various Number of Solvent  
Molecules in the Unit Cell of the Extended Structure  
(Four Chains per Cell)

solvent	density, g·cm <sup>-3</sup>		
	4	8	16
hexahydroindan	0.865	0.943	1.099
nitrobenzene	0.864	0.942	1.097
decalin	0.873	0.960	1.134
cyclooctane	0.857	0.928	1.069

rigorous solvent exchange with a low-boiling solvent. The calculated densities with varying number of solvent mol-

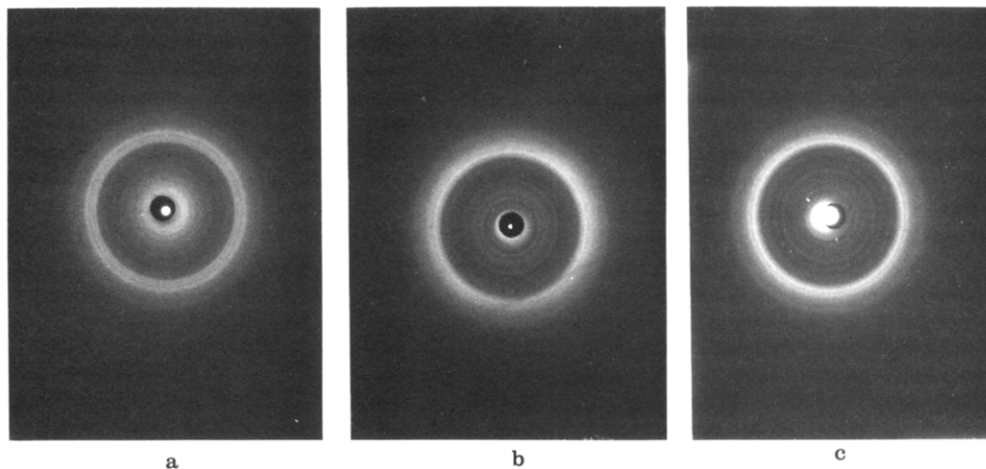


**Figure 2.** X-ray diffraction patterns from iPS films after exposure to vapors of (a) hexahydroindan (3 days), (b) nitrobenzene (5 days), and (c) cyclooctane (24 h).

ecules in the unit cell are given in Table III.

It is known that the fraction  $x_c$  of crystalline material in a semicrystalline sample can be calculated by using the equation<sup>17</sup>

$$x_c = \frac{\rho_c}{\rho} \left( \frac{\rho - \rho_a}{\rho_c - \rho_a} \right) \quad (1)$$

where  $\rho$  is the measured density of the semicrystalline film and  $\rho_a$  and  $\rho_c$  correspond to the totally amorphous and crystalline materials, respectively. In the present case, with the extended conformation,  $\rho$  varies from 1.028 to 1.034 for the solvent-exposed films (Table I). The fraction  $x_c$  can be calculated if the density  $\rho_c$  of the crystalline extended conformation is known and vice versa. Although the crystallinity has not been measured in this study, it would be useful to calculate  $\rho_c$  for a range of values of  $x_c$ . The purpose of this exercise is to simply get some idea of the range of density for the perfectly crystalline extended conformation. With this in mind, using values of  $\rho = 1.034 \text{ g}\cdot\text{cm}^{-3}$  and  $\rho_a = 1.05 \text{ g}\cdot\text{cm}^{-3}$  in eq 1, we find that the value of  $\rho_c$  varies from 0.974 to 1.32  $\text{g}\cdot\text{cm}^{-3}$  as  $x_c$  varies from 0.2 to 0.9. Thus, clearly, the density of the extended form is lower than that of the crystalline form of the threefold helical structure. It is also slightly lower than that of the amorphous iPS. Although the reason for this is not clear at this stage, the inefficient packing and voids in the unit cell created by the presence of bulky solvent molecules might contribute to this effect. The extended conformation can therefore be termed the low-density crystalline form of iPS. On the basis of the measured densities given in Table I and the above discussion, a four-chain unit cell with 8–16 solvent molecules appears to be a satisfactory representation of this crystalline form.

The X-ray pattern from the film exposed to ethylbenzene is shown in Figure 3. It is seen that only the reflections corresponding to the threefold helical structure are present, and not the extended conformation. This is similar to the results obtained in the gelation experiments,<sup>10</sup> in which ethylbenzene promoted gels containing only the threefold helical form. Thus, the presence of bulky hydrocarbons or certain types of substituted aromatics, e.g., nitrobenzene, is required for the crystallization of the extended form.

**Solvent Exposure of Semicrystalline Films.** The crystallization of the extended conformation upon exposure of amorphous films to the vapor of bulky solvents shows that significant portions of the chains exist in the non-staggered *tt* state. Further, the observation that the crystallization occurs not by annealing but only upon vapor

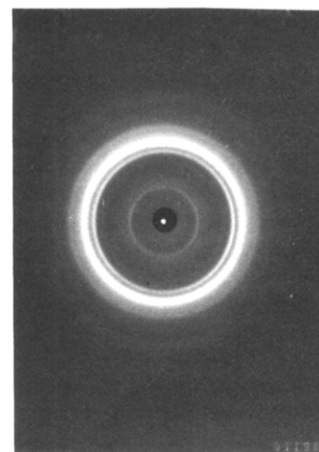


**Figure 3.** X-ray diffraction pattern from iPS film after exposure to ethylbenzene vapor for 5 days.

exposure shows that intercalation of solvent molecules between the chains is required in order to provide the necessary intermolecular interaction.

If the intramolecular energy of the extended conformation is as favorable as the theoretical calculations predict,<sup>1</sup> it is possible that in the semicrystalline films (crystallized by annealing) containing the threefold helical form, the chains in the amorphous parts of the film exist, to an appreciable extent, in the extended conformation. In such an event it should be possible to crystallize such a conformation by exposure of a semicrystalline film to solvent vapor.

An amorphous film of sample B obtained by melt-quenching was annealed at 200 °C for 1 h. The X-ray pattern from such a film, shown in Figure 4a, contains reflections corresponding to the threefold helical form. This semicrystalline film was then exposed to hexahydroindan vapor for 3 days at room temperature. The X-ray pattern recorded after vapor exposure is shown in Figure 4b. It is clearly seen that crystallization of the extended form has been achieved in this film, as exhibited by the presence of the 5.1-Å reflection.

Figure 5a shows the X-ray pattern from an oriented film, obtained by annealing an amorphous film under tension. The reflections correspond to the threefold helical form. Upon exposure of this oriented film under tension to hexahydroindan vapor, the pattern shown in Figure 5b is obtained. The appearance of the meridional reflection characteristic of the extended conformation confirms that the latter has crystallized.

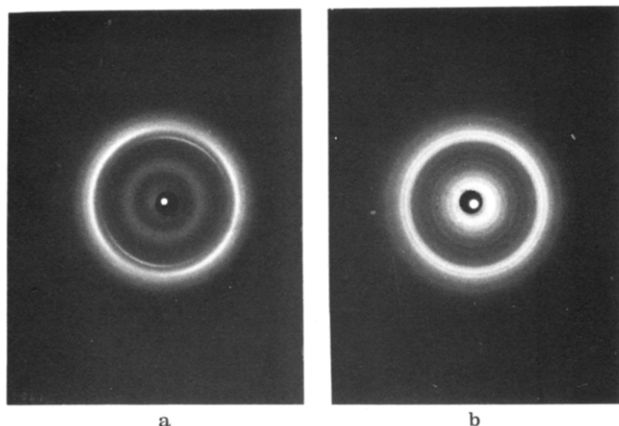


**Figure 4.** X-ray diffraction pattern from (a) semicrystalline iPS film containing the threefold helical structure and (b) after exposure to hexahydroindan vapor for 3 days. Note the reflection characteristic of the extended conformation in (b).

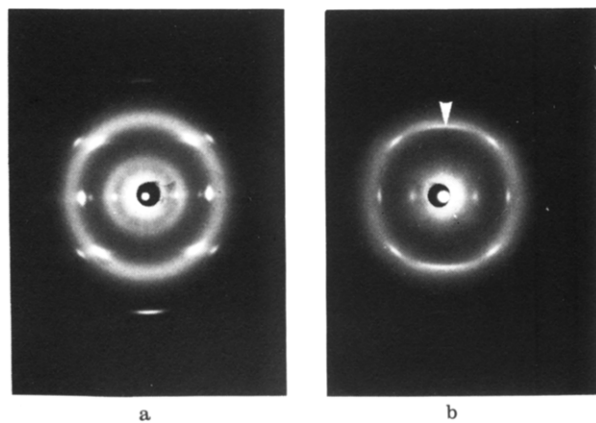
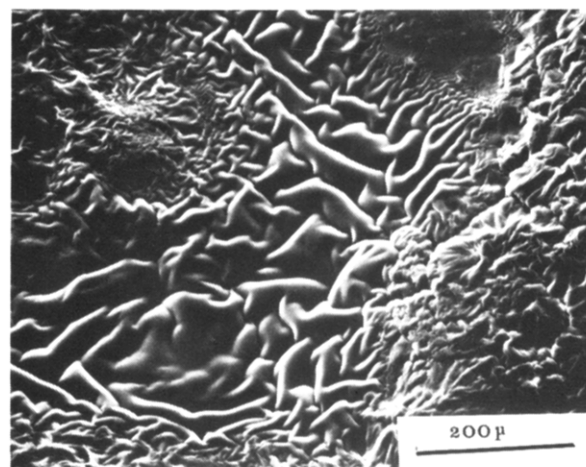


**Figure 5.** X-ray diffraction pattern from (a) an oriented semicrystalline iPS film containing the threefold helical structure and (b) after exposure to hexahydroindan vapor for 3 days. The meridional reflection, characteristic of the extended conformation, is marked in (b).

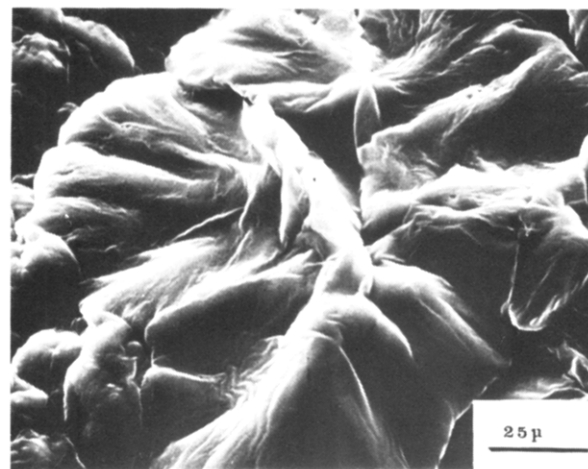
The crystallization upon vapor exposure of the extended conformation in semicrystalline film already containing the threefold helical structure shows that the former is indeed present in semicrystalline films and that solvent molecules are required to provide the necessary stabilization for crystallization. In the absence of solvent molecules, the extended conformation constitutes a significant portion of the amorphous domains of the semicrystalline film. These observations confirm that the extended conformation is accessible to the iPS chain. In addition, it is clear that the perpetuation of the nonstaggered *tt* conformation along the chain is also significant so as to be sufficient for crystallization. Although crystallite size measurements have not been made here, it is obvious that at least a few turns of the extended helix are required for crystallization to occur.

The measurement of the meridional reflection in Figure 5b shows that its spacing is 5.0 Å rather than 5.1 Å. This would tend to reduce the repeat distance along the chain to 30 Å. This would obviate the struggle, that was necessary in previous studies<sup>1,8</sup> to distort the skeletal bond angles to account for the repeat distance of 30.6 Å. Further measurements on well-oriented films are necessary to confirm the reduction in the repeat distance.

Upon annealing in the range 80–120 °C (depending on the solvent), the extended conformation melts and the threefold helical structure appears. It was shown before<sup>10</sup> that these two events are independent; i.e., the extended conformation does not transform itself continuously to the



a



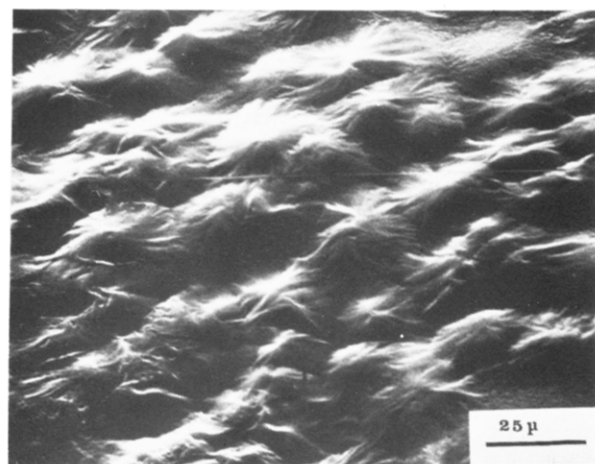
b

**Figure 6.** SEM of the spherulitic morphology in a melt-quenched film of sample B (see text) after exposure to hexahydroindan vapor for 3 days.

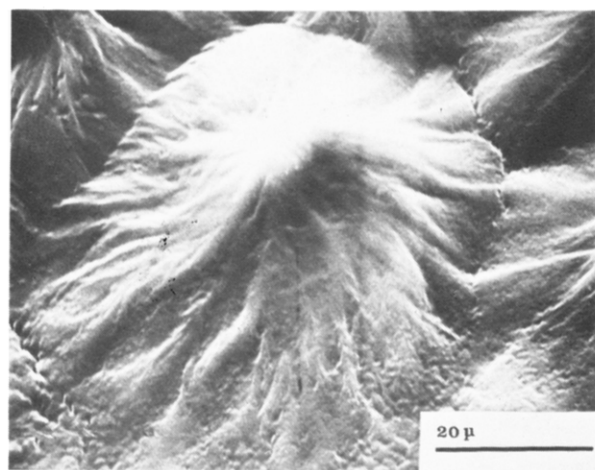
threefold helix. The fact that the extended conformation can be crystallized even after the formation of the threefold helical structure tends to support this conclusion.

**Microscopy.** Scanning electron microscopy was mainly used to observe the morphology of the solvent-exposed films of iPS. A view of the melt-quenched film of sample B (initially crystalline powder) exposed to hexahydroindan vapor for 3 days is shown in Figure 6. Here, Figure 6a contains large sheaflike spherulitic structures of the order of 180–200 μm in size, and these are connected by ribbed lamellar ridges. These ridges are observed commonly in solvent-exposed films of iPS (see below). They are present in films exposed to the various solvents used here, irrespective of whether the initial film was melt quenched or solution cast. Microscopic observations of films exposed for varying lengths of time as well as after different periods of drying under ambient conditions were consistent. Thus we believe that these ridges represent the inherent morphology and are not due to causes such as film shrinkage. An enlarged view of one of the spherulites is shown in Figure 6b. Within the sheaflike structure, there are striations or ridges of the order of 0.6 μm. The spherulitic nature was confirmed by observing the morphology under cross polaroids in an optical microscope. Upon annealing of the film at 80–120 °C, the spherulitic structure and the ridges are lost, confirming that these correspond to the extended conformation. Compared to this sample, the initially amorphous sample A when melt cast and exposed





a



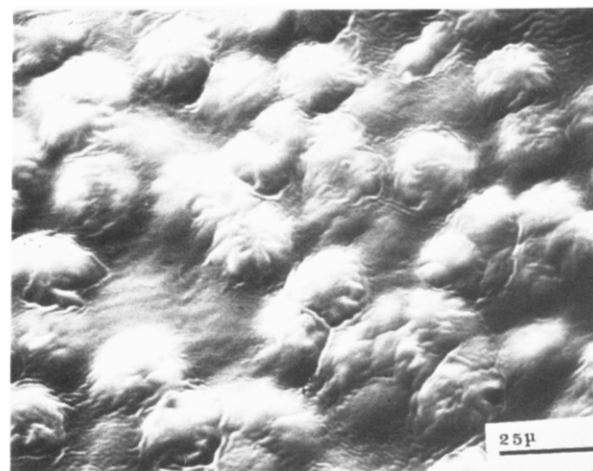
b

**Figure 7.** SEM micrographs of a melt-quenched film of sample A (see text) after exposure to hexahydroindan vapor for 3 days.

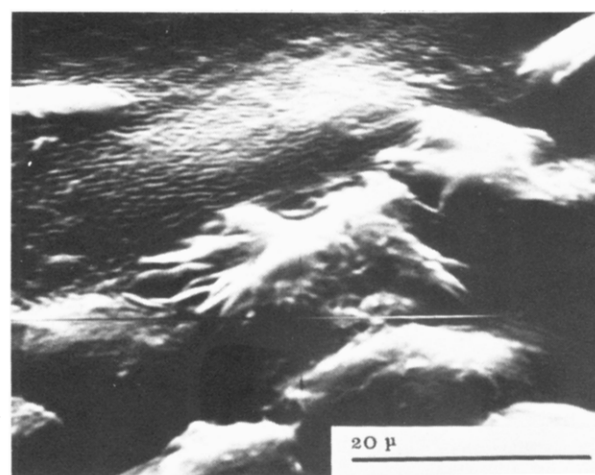
to hexahydroindan for 3 days showed smaller spherulitic structures. Figure 7 shows the SEM micrographs. It is seen that dendritic structures of the order of 20–30  $\mu\text{m}$  in diameter are found in profusion. The enlarged view in Figure 7 shows the fine line of discontinuity between two spherulites. Here again, similar to Figure 6, thin lamellar structures of the order of 0.3–0.6  $\mu\text{m}$  are seen radiating from the center of the spherulite.

The growth of the spherulites seems to be dependent on the initial starting material. The difference in size observed above between the spherulites in Figures 6 and 7 could be due to the difference in thickness of the films and the resultant variations in the diffusion rate. No attempt was made here to control the thickness of the films. The growth rate and size of the spherulites could also be influenced by the atactic content.<sup>18</sup> However, in this case, the NMR analysis showed the isotactic dyad content to be similar in both samples A and B. Hence, contribution to the variation in spherulite size from the difference in the tacticity should only be minimal in this case, unless higher order effects such as those due to pentad and hexad sequences differ in samples A and B. Further, determining whether the atactic material rejected during the spherulitic growth is contained in the interfibrillar or interlamellar regions would require a detailed study of the spherulitic size with samples of different atactic content.

Differences in morphology are also observed between the melt-cast films and those prepared from toluene solution.



a



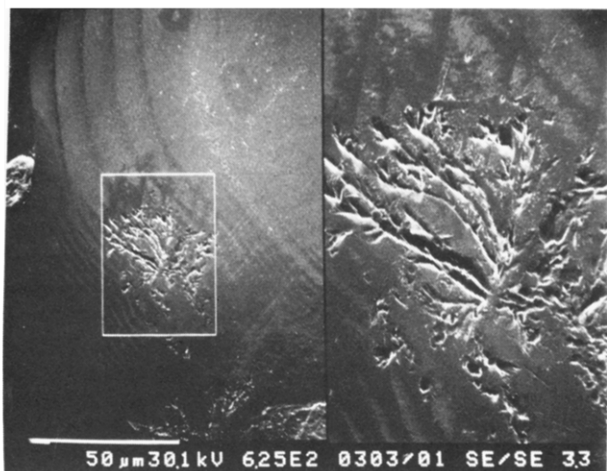
b

**Figure 8.** SEM micrographs of a toluene-cast film of sample B after exposure to hexahydroindan vapor for 8 days.

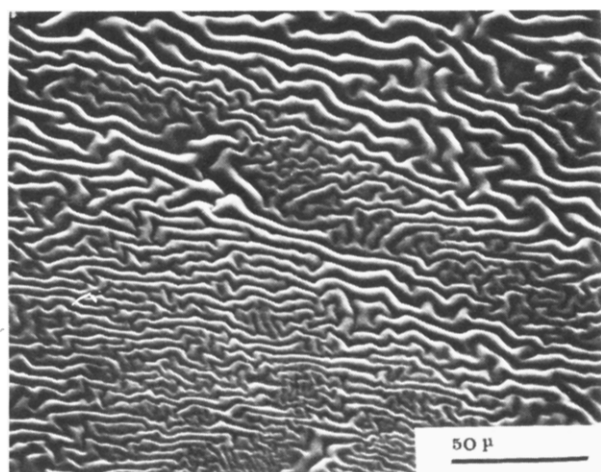
Figure 8 shows the dendritic structures formed upon exposing a film of sample B prepared from toluene solution to hexahydroindan for 8 days. These dendrites are fairly uniform in size, of the order of 20  $\mu\text{m}$  in diameter. The “ribbed” ridges are also evident. Figure 8a shows a boundary line surrounding most of the dendrites, and Figure 8b shows an enlarged view of one of the dendrites. It is seen that these structures are poorly formed compared to those observed with melt-cast films. Apart from thickness variations, the presence of any residual toluene in the films could also contribute to this difference.

Figure 9 shows the micrograph of sample B (toluene film) exposed to hexahydroindan for 8 days and subsequently annealed at 125  $^{\circ}\text{C}$  for 1 h. This seems to be the remnants of a partially melted dendritic structure as seen in Figure 8b. Almost continuous “spines” of 150- $\mu\text{m}$  length are seen, with all the interspinal material molten.

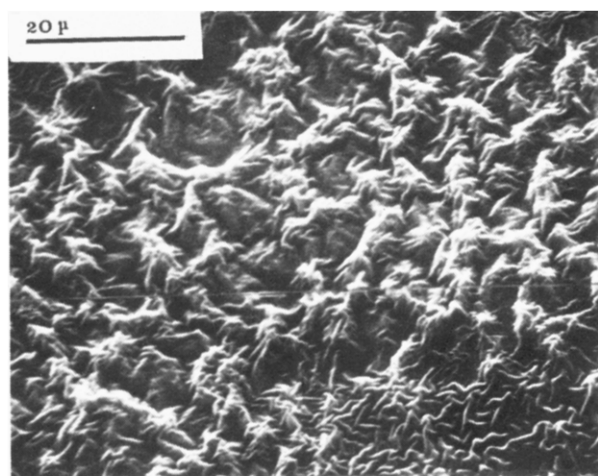
Figure 10 shows the micrographs obtained for toluene-cast films of samples A and B exposed to nitrobenzene for 5 days. The ribbed ridges are predominant in Figure 10a and the dendritic structures in Figure 10b. The ribbed ridges are also present in the lower left-hand corner of Figure 10b. It would seem that the ridges are an advanced state of the spherulitic growth. Figure 11 shows the micrograph of the toluene-cast film of sample A exposed to hexahydroindan for 18 days. Comparing with Figures 6 and 7, it is seen that extended exposure causes the formation of ridges and, as such, these can be considered to



**Figure 9.** SEM micrograph of sample shown in Figure 8 after annealing at 125 °C for 1 h. The partially molten spherulite is seen. The micrograph at the right is a 3.3 $\times$  magnified view of that at the left.



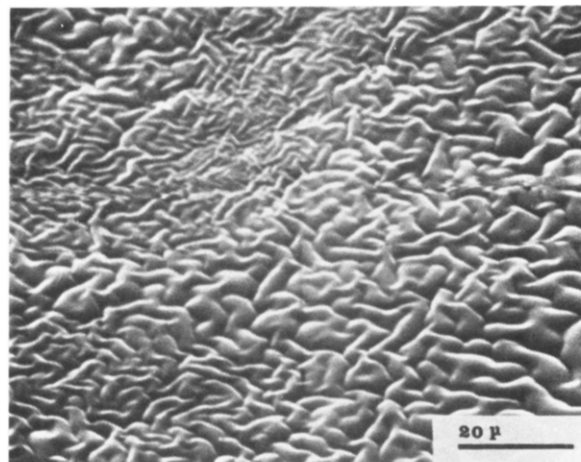
a



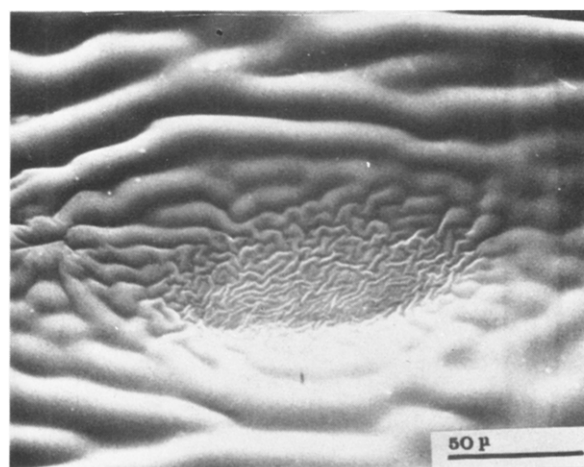
b

**Figure 10.** SEM micrograph of toluene-cast films of (a) sample A and (b) sample B after exposure to nitrobenzene vapor for 5 days.

be the postspherulitic formation. Upon annealing of the film seen in Figure 10a at 125 °C for 3 h, melting of the ridges is observed, as shown in Figure 12. Ridges as in Figure 10a are seen with the toluene-cast film of sample A after exposure to cyclooctane vapor for 24 h, as in Figure 13.



a



b

**Figure 11.** SEM micrograph of a toluene-cast film of sample A after exposure to hexahydroindan vapor for 18 days.

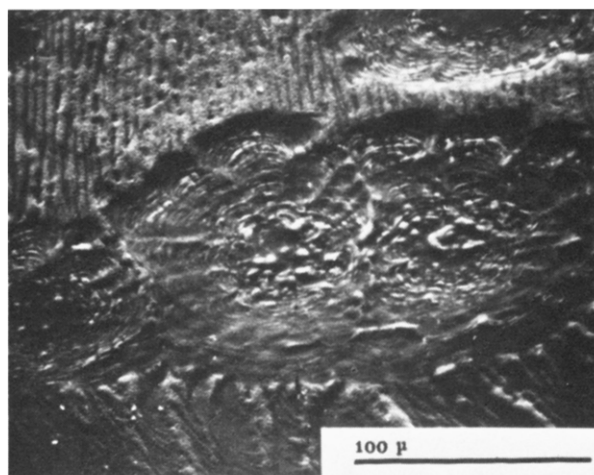


**Figure 12.** SEM micrograph of the film shown in Figure 10a after annealing at 125 °C for 3 h.

It was stated above that the films exposed to ethylbenzene did not contain the extended conformation but only the threefold helical structure. A micrograph of such a film is shown in Figure 14. Neither the dendritic nor the ridge structure is seen here, but almost parallel lamellar periodicity is observed. The micrograph, in fact, shows three substructures: the parallel lamellae, about 1  $\mu$ m thick, are disposed in bands, about 20–30  $\mu$ m wide. Close observation of the 1- $\mu$ m lamellae shows that these are

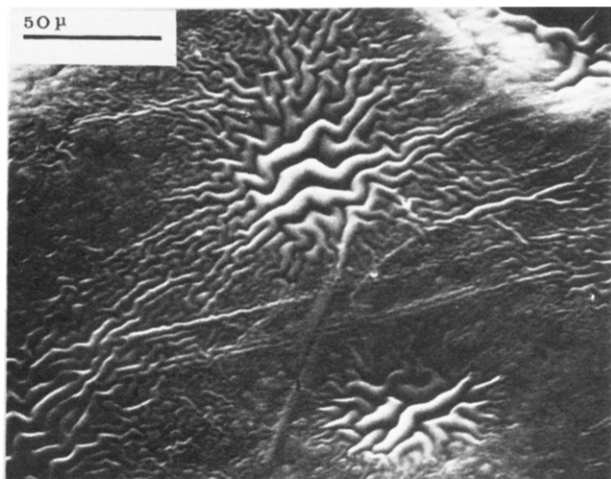


**Figure 13.** SEM micrograph of a toluene-cast film of sample A after exposure to cyclooctane vapor for 24 h.

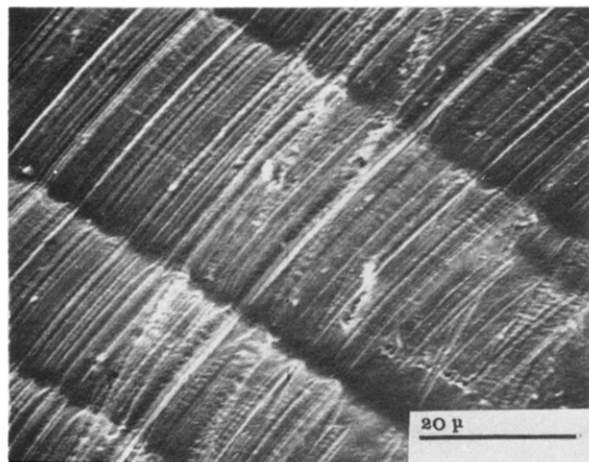


**Figure 14.** SEM micrographs of a toluene-cast film of sample A after exposure to ethylbenzene vapor for 5 days.

striated, at intervals of 1  $\mu\text{m}$  normal to their length.

### Conclusions

The presence of the extended conformation in iPS has been established by the present studies on the solvent-exposed films. The observation that by proper choice of solvent molecule either the extended or the threefold helical conformation can be crystallized at room temperature shows that the former constitutes the amorphous portions of the crystalline films of iPS containing the threefold helical structure and vice versa. The perpetuation of the chain in the extended conformation is significant. Due to the predominant intramolecular interaction present in such a conformation, solvent molecules are necessary to provide the stability required for the crystallization. Further, the fact that crystallization of the extended conformation can be achieved at room temperature by solvent exposure shows that it is not an unstable conformation, at least in the intramolecular sense. Hence, its lower melting temperature compared to that of the threefold helical structure could be attributed to collapse of the intermolecular interaction upon removal of the solvent molecule. Since the melting of the extended form and the crystallization of the threefold helical structure are independent events at intermediate temperatures, both forms can coexist in various proportions. Such studies on the relative proportions will be reported in due course.

The preference for the nonstaggered *tt* state has hitherto been neglected in the interpretation of the solution behavior of iPS. Perhaps inclusion of such states in the

computation of the unperturbed dimensions would account for the measured temperature dependence of the characteristic ratio of the unperturbed end-to-end distance of iPS in an atactic polystyrene matrix.<sup>19</sup> Further, consideration of the short-range intramolecular interaction, as in the extended conformation, in addition to the intrachain long-range segmental interaction becomes important in understanding the behavior of iPS in poor solvents.

The anomalous temperature dependence of solution and bulk properties of iPS and aPS and the transition at about 80 °C have been interpreted in terms of a transition between the threefold helical structure and the random coil.<sup>20,21</sup> Recent NMR studies attribute the behavior to increased motion of the side groups.<sup>22</sup> It is likely that the first-order transition in solution observed in these experiments is due, at least in part, to the change in the phenyl-solvent interaction and the relative preference for the threefold and extended helical conformations.

Overbergh et al.<sup>23</sup> and Faulkner et al.<sup>24</sup> have previously observed the crystallization of amorphous iPS films upon exposure to solvent vapor. The former authors exposed melt-quenched amorphous films to dichloromethane and acetone. Faulkner et al.<sup>24</sup> used films cast from a solution of iPS in mesitylene and *o*-chlorotoulene, which were subsequently exposed to *n*-hexane. Overbergh et al.<sup>23</sup> reported that an unstable intermediate crystalline structure is formed, which transforms to a more stable phase upon annealing at  $\sim 150$  °C. On the basis of X-ray data, they concluded that a reorganization of the crystallites rather than recrystallization occurred. On the basis of this and the fact that bulky cyclic hydrocarbons are required to crystallize the extended conformation, we believe that the intermediate crystalline structure reported by Overbergh et al. does not correspond to the extended conformation.

It has also been shown here that the extended conformation forms dendritic structures. The differences in size and formation observed here could be due to the differences in thickness of the films, residual solvent in toluene-cast films, and so on. In addition, the observation that the ridges formed when exposing the films to hexahydroindan for 18 days or to cyclooctane for 24 h, shows that the nature of the solvent molecule interaction is an important factor. It should be added that our initial attempts to crystallize the films with decalin vapor at room temperature have been unsuccessful. It is believed that both the time of exposure and temperature are important parameters. A detailed study of these effects will be reported in due course.

### References and Notes

- (1) Sundararajan, P. R. *Macromolecules* **1979**, *12*, 575.
- (2) Natta, G.; Corradini, P.; Bassi, I. W. *Nuova Cimento, Suppl.* **1960**, *15*, 68.
- (3) Sundararajan, P. R.; Flory, P. J. *J. Am. Chem. Soc.* **1974**, *96*, 5025.
- (4) Sundararajan, P. R. *Macromolecules* **1977**, *10*, 623. *Ibid.* **1978**, *11*, 256. *Ibid.* **1980**, *13*, 512.
- (5) Kusanagi, H.; Tadokoro, H.; Chatani, Y. *Macromolecules* **1976**, *9*, 531.
- (6) Atkins, E. D. T.; Isaac, D. H.; Keller, A.; Miyasaka, K. *J. Polym. Sci., Polym. Phys. Ed.* **1977**, *15*, 211.
- (7) Atkins, E. D. T.; Isaac, D. H.; Keller, A. *J. Polym. Sci., Polym. Phys. Ed.* **1980**, *18*, 71.
- (8) Corradini, P.; Guerra, G.; Petraccione, V.; Pirozzi, B. *Eur. Polym. J.* **1980**, *5*, 1089.
- (9) Lovell, R.; Windle, A. H. *J. Polym. Sci., Polym. Lett. Ed.* **1980**, *18*, 67.
- (10) Sundararajan, P. R.; Tyrer, N. J.; Bluhm, T. *Macromolecules* **1982**, *15*, 286.
- (11) Yoon, D. Y.; Sundararajan, P. R.; Flory, P. J. *Macromolecules* **1975**, *8*, 776.
- (12) Wellinghoff, S.; Shaw, J.; Baer, E. *Macromolecules* **1979**, *12*, 932.



- (13) Nieduszynski, I. A.; Marchessault, R. H. *Biopolymers* 1972, 11, 1335.
- (14) Shepherd, L.; Chen, T. K.; Harwood, H. J. *Polym. Bull.* 1979, 1, 445.
- (15) Natta, G.; Corradini, P. *Makromol. Chem.* 1955, 16, 77.
- (16) Atkins, E. D. T.; Keller, A.; Shapiro, J. S.; Lemstra, P. J. *Polymer* 1981, 22, 1161.
- (17) Alexander, L. E. "X-ray Diffraction in Polymer Science"; Wiley-Interscience: New York, 1969; p 189.
- (18) Keith, H. D. *J. Polym. Sci., Part A* 1964, 2, 4339.
- (19) Guenet, J. M.; Picot, C.; Benoit, H. *Macromolecules* 1979, 12, 86.
- (20) Reiss, C.; Benoit, H. C. R. *Hebd. Seances Acad. Sci.* 1961, 256, 268.
- (21) Liu, K.-J.; Ullman, R. *Polymer* 1965, 6, 100.
- (22) Inoue, Y.; Konno, T. *Polym. J.* 1976, 8, 457.
- (23) Overbergh, N.; Berghmans, H.; Smets, G. *Polymer* 1975, 16, 703. *Ibid.* 1978, 19, 602.
- (24) Faulkner, D. L.; Hopfenberg, H. B.; Stannett, V. T. *Polymer* 1977, 18, 1130.

## Crystal Structure of Pristine and Iodine-Doped *cis*-Polyacetylene

James C. W. Chien\* and Frank E. Karasz\*

Department of Polymer Science and Engineering, Department of Chemistry,  
Materials Research Laboratory, University of Massachusetts,  
Amherst, Massachusetts 01003

Kaoru Shimamura

Institute for Chemical Research, Kyoto University, Uji 611, Japan.  
Received November 4, 1981

**ABSTRACT:** Acetylene has been polymerized directly onto the electron microscope grid at  $-78^{\circ}\text{C}$  to produce ultrathin films of *cis*-(CH) $_x$  having regions of oriented fibrils. An electron beam directed at these fibrils gave fiber electron diffraction patterns. Pristine *cis*-(CH) $_x$  has an orthorhombic unit cell with  $a = 7.68$ ,  $b = 4.46$ , and  $c = 4.38$  Å. The fiber and molecular axes are along  $c$ . The space group is *Pnam*, with a setting angle of  $31$ – $33^{\circ}$  for the *cis*-transoid structure and  $34$ – $36^{\circ}$  for the *trans*-cisoid structure. The structure contains nonbonded interactions between some of the atoms in the unit cell. *cis*-(CH) $_x$  doped by iodine to the semiconducting state showed all the unperturbed reflections of undoped *cis*-(CH) $_x$ . In addition, there are present meridional reflections of undoped *trans*-(CH) $_x$  and new ones arising from the doped structure. Heavily iodine-doped metallic polyacetylene had electron diffraction entirely different from that of the undoped polymers. A structure is proposed for this material.

### Introduction

Acetylene can be polymerized as predominantly *cis*-(CH) $_x$  or *trans*-(CH) $_x$  under proper conditions,<sup>1–3</sup> the latter being the thermodynamically more stable isomer. In fact, *cis*-(CH) $_x$  can be readily isomerized to *trans*-(CH) $_x$  by heating in vacuo.<sup>2–5</sup> Pristine *cis*-(CH) $_x$  is free of unpaired spins<sup>6</sup> when polymerized at  $-78^{\circ}\text{C}$ . Upon warming up to room temperature, there is some isomerization,<sup>4</sup> producing about one neutral soliton per 25 000 CH units. The polymer is flexible and can be stretched about threefold. *cis*-(CH) $_x$  has a room-temperature conductivity<sup>7</sup> of ca.  $10^{-9}$  ( $\Omega\text{ cm}$ ) $^{-1}$ . By comparison, *trans*-(CH) $_x$  is brittle, contains one soliton per 1000–3000 CH units, and has a room-temperature conductivity of  $10^{-5}$  ( $\Omega\text{ cm}$ ) $^{-1}$ . Knowledge of their structures is essential to the understanding of the properties of polyacetylene.

We have developed a method to prepare very thin films ( $\sim 1000$  Å) directly on the electron microscope grid.<sup>8</sup> By repeated washing of the polymer and evaporation of solvent, there were formed regions of oriented bundles of polyacetylene fibrils. Analysis of the electron diffraction from these oriented fibrils yielded the crystal structure of *trans*-(CH) $_x$ .<sup>9</sup>

The crystal structure of undoped *cis*-(CH) $_x$  was first studied by Baughman et al. with X-ray diffraction<sup>10</sup> on randomly oriented specimens. Ten reflections were observed; seven of them are very broad. Together with packing calculations, Baughman et al. concluded that the unit cell is orthorhombic, containing two molecules and a *Pnam* space group. Lieser et al.<sup>11</sup> reported electron diffraction results on *cis*-(CH) $_x$ . Only equatorial reflections

were observed at normal electron beam incidence. Upon tilting of the specimen, the (001) and (221) reflections become observable. The two studies agreed in the unit cell dimensions. They differ in the indexing of reflections. Lieser et al.<sup>11</sup> stated that their samples have a space group different from *Pnam*, a folded-chain morphology, and the  $c$  axis (molecular axis) perpendicular to the axis linking the lamellae ("fiber" axis). Baughman et al. assigned the  $b$  axis to be the molecular chain axis.

Because of the above-mentioned discrepancies in the *cis*-(CH) $_x$  structure, we have now carried out electron diffraction studies on oriented fibrils of this polymer. The results are in agreement with the X-ray work, except that the  $c$  axis has been identified unambiguously to be the molecular axis and the fiber axis as well. Therefore, the previous  $b$ - and  $c$ -axis assignments by Baughman et al.<sup>10</sup> should be interchanged.

In addition, *cis*-(CH) $_x$  has been doped to both the semiconducting state and the metallic state with iodine. Structures for these materials are also described.

### Experimental Section

The procedure for in situ acetylene polymerization has been described previously.<sup>8,9</sup> The semiconducting polymer (A) was obtained by doping with  $\text{I}_2$ ; both the specimen and the iodine were maintained at  $-23^{\circ}\text{C}$  ( $p_{\text{I}_2} = 3 \times 10^{-3}$  mm) for 4 h. *cis*-(CH) $_x$  was heavily doped with iodine to the metallic conducting state (B) by keeping the polymer and iodine at  $10^{\circ}\text{C}$  overnight ( $p_{\text{I}_2} = 8.08 \times 10^{-2}$  mm).

A JEOL 100CX EM diffractometer was used in this investigation. The sample was first examined in the transmission mode. Electron diffraction patterns of selected regions of the oriented